The minimizing of pressure losses in a fan drift-mine shaft intersection, using computational fluid dynamics

Josua P. Meyer[1] and **Wynand M. Marx**[1]
(First received April 1993; Final version July 1993)

Abstract

Working conditions in deep mining have to be made acceptable for human beings by ventilating the working areas with cooled air. In some instances, chilled air is blown from the surface level, via a ventilation duct, or fan drift, down a vertical mine shaft to the working areas. Inadequate aerodynamic properties at the fan drift-mine shaft intersection can result in high pressure losses across the intersection. As no definite set of rules exists for designing the optimum intersection, and scale model testing has been the only optimization tool available hitherto, the need for a fast, economically viable and accurate method motivated the present optimization study, using Computational Fluid Dynamics (CFD). The optimization is done through a parametric study, resulting in 40 different intersection geometries to be analysed. The flow field is solved, for the various geometries, with an industrial CFD code. Up to 28% reduction in pressure loss across the intersection was predicted with the limited parameter settings of a parametric study, promising significant savings in fan power-cost. The study highlighted the effectiveness of CFD in solving industrial air-flow problems and a functional set of data is introduced to fan drift designers to both design and optimize fan drift-mine shaft intersections.

Introduction

High rock temperatures in deep mining situations create a need for ventilation of working areas with cooled air by using a refrigeration plant situated at surface level, the air having to be transported to the working areas via a ventilation duct joining the shaft beneath the bank level, as illustrated in Figure 1. The intersection of this ventilation duct, or fan drift, with the shaft is important in the sense that inefficient aerodynamic geometries at such an intersection can cause various flow-related problems. Some of the major problems are high fan-power cost due to high pressure loss across the intersection, the spillage of chilled air to the atmosphere through the top of the shaft and high cross-wind speeds in the shaft which make the slinging of long material underneath a cage dangerous as the material may be deflected into steel work within the shaft.

[1]Department of Mechanical Engineering, Potchefstroom University for CHE, Private Bag X6001, Potchefstroom, 2522 Republic of South Africa

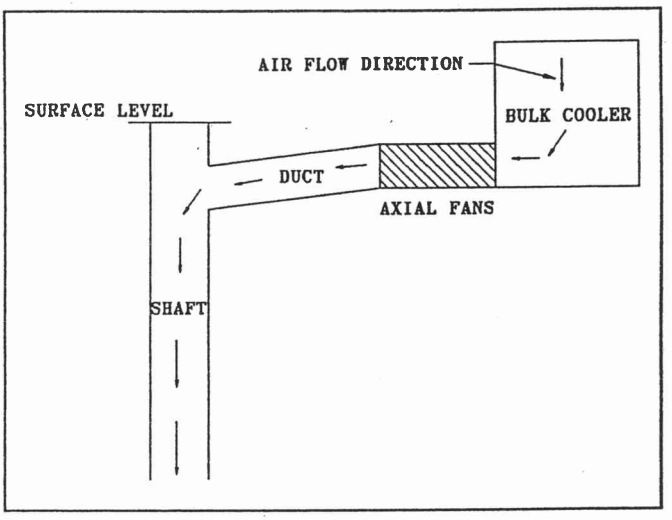

Figure 1. A typical mine ventilation duct.

In this paper we consider a numerical investigation, in the form of a parametric study, to determine the influence of different geometry parameters on the pressure loss across a typical ventilation duct-mine shaft intersection, using Computational Fluid Dynamics (CFD). The study was done on an existing mine shaft-fan drift intersection, namely, Number 6 North Shaft at Hartebeestfontein Gold Mining Company Limited (HGM), which is taken as a typical intersection and not because of any problems being experienced at this specific intersection. The aim of the study was to accumulate a set of data to assist designers in the selection of the optimum geometry parameters in future fan drift designs and to show the tendencies of the flow for different geometries to create a better understanding of flow behaviour in existing intersections. The effective application of CFD in large industrial air-flow problems was a secondary goal of this study.

A thorough literature survey revealed no similar study to this in the past. Published literature dating from 1962 to 1990 showed that optimization of pressure losses in fan drift-mine shaft intersections is done by experimental or by scale-model testing.[1;2;3;4;5] This survey also showed that the design of such intersections is done by rule-of-thumb and that, although aerodynamics are not overlooked, geometries are designed with low capital expenditure as primary objective. Accordingly, no definite rule or method exists for designing an efficient duct-shaft intersection.[5]

The outline of this paper is as follows. Modelling of the intersection is initially discussed whereafter numerical simulation of the flow field is described. The results are presented in graphs and the tendencies of the different geometries, regarding pressure loss across the intersection, are discussed. The financial impact of the change in pressure loss, in terms of fan-power cost, is also discussed.

Modelling of the fan drift-mine shaft intersection

The variable geometry parameters chosen for the parametric study are illustrated in Figure 2. The different settings of these parameters, ϕ, θ, and L, are taken as ratios of the original dimensions of the existing intersection geometry (HGM). These settings are chosen to be 0, 0.5, 1, and 1.5 times the original dimensions, producing 64 combinations. If the impractical and repeated combinations are omitted, the number of settings reduces to 40, as tabulated in Table 1. The original dimensions of the typical intersection are $\phi = 45°$, $\theta = 6.8°$, and $L = 4.15$ m.

Table 1 Case studies (subscript 0 denotes original)

Case	L/L_0	θ/θ_0	ϕ/ϕ_0	Case	L/L_0	θ/θ_0	ϕ/ϕ_0
1	0	0	0	**21**	1	0.5	1
2	0	0.5	0	**22**	1	0.5	1.5
3	0	1	0	**23**	1	1	0.5
4	0	1.5	0	**24**	1	1	1
5	0.5	0	0.5	**25**	1	1	1.5
6	0.5	0	1	**26**	1	1.5	0.5
7	0.5	0	1.5	**27**	1	1.5	1
8	0.5	0.5	0.5	**28**	1	1.5	1.5
9	0.5	0.5	1	**29**	1.5	0	0.5
10	0.5	0.5	1.5	**30**	1.5	0	1
11	0.5	1	0.5	**31**	1.5	0	1.5
12	0.5	1	1	**32**	1.5	0.5	0.5
13	0.5	1	1.5	**33**	1.5	0.5	1
14	0.5	1.5	0.5	**34**	1.5	0.5	1.5
15	0.5	1.5	1	**35**	1.5	1	0.5
16	0.5	1.5	1.5	**36**	1.5	1	1
17	1	0	0.5	**37**	1.5	1	1.5
18	1	0	1	**38**	1.5	1.5	0.5
19	1	0	1.5	**39**	1.5	1.5	1
20	1	0.5	0.5	**40**	1.5	1.5	1.5

The number of geometries may seem restrictive but the computer time, and thus cost, must be taken into account. A more refined and detailed study can be done if the initial study shows the possibility of large savings which will justify further studies. Because of the symmetry of the flow domain, only half of the geometry had to be modelled which reduced the number of nodes and the computation time by half. The computational mesh consists of approximately 11 000 node points which resulted in a relatively course grid for this size of geometry. As the flow tendencies for different geometries are to be compared, and computer time had to be taken into account, this number of nodes is significant. The boundary condition at the top of the shaft is difficult to specify as the direction of the flow at this point is unknown, i.e. the flow can be either into the shaft or outward to the atmosphere. To overcome this difficulty, a plenum is modelled at the top of the shaft so that the flow at the actual boundary can thus behave naturally. A zoomed view of the computational mesh at the intersection can be seen in Figure 3, where the plenum is shown at the top of the shaft. Through numerical experimentation it was found the only 76 m of the shaft is needed to be modelled as the gradients of the flow did not alter significantly beyond this point.

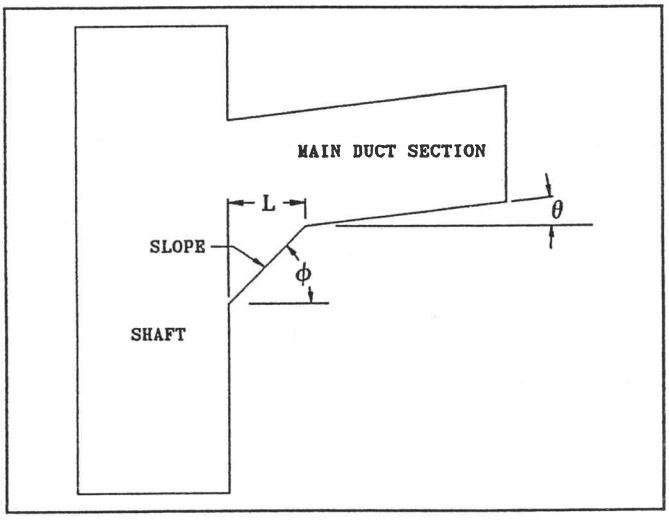

Figure 2. Geometry variables.

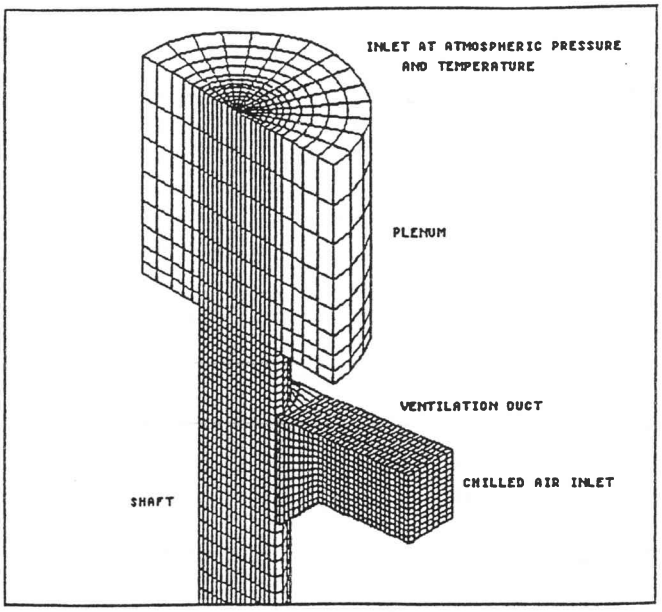

Figure 3. The computational mesh.

Simulation of the flow field

An industrial CFD code written by Computational Dynamics Ltd, namely STAR-CD, was used to simulate the flow field through the intersection. The governing partial differential equations of fluid flow and heat transfer are solved by the STAR-CD code by marching through the computational mesh in space and time. For the purposes of this study, the equations describing the conservation of mass and momentum are solved. These equations are given as:

Conservation of mass:

$$\frac{1}{\sqrt{g}}\frac{\partial}{\partial t}(\sqrt{g}\,\rho) + \frac{\partial}{\partial x_j}(\rho\, u_j) = 0 \qquad (1)$$

Conservation of momentum:

$$\frac{1}{\sqrt{g}}\frac{\partial}{\partial t}(\sqrt{g}\,\rho\, u_i) + \frac{\partial}{\partial x_j}(\rho\, u_j\, u_i + \tau_{ij}) = \frac{\partial p}{\partial x_i} + s_i \qquad (2)$$

where $t \equiv$ time; $x_i \equiv$ Cartesian coordinate $(i = 1, 2, 3)$; $u_i \equiv$ absolute fluid velocity component in direction x_i; $u_j \equiv u_j - u_{cj}$, relative velocity between fluid and local (moving) coordinate frame which moves with velocity u_{cj}; $p \equiv$ piezometric pressure $= p_s + \rho_0 g_m x_m$ where ρ_s is static pressure, ρ_0 is reference density, the g_m are gravitational field components and the x_m are coordinates from a datum; $\rho \equiv$ density; $\tau_{ij} \equiv$ stress tensor components; $s_i \equiv$ momentum source components; $\sqrt{g} \equiv$ determinant of metric tensor; and repeated subscripts denote summation.

The well known SIMPLE algorithm is used with a finite volume approach to solve the equations. The turbulence model used in this study is the k-epsilon model which, together with the SIMPLE algorithm, is described in the STAR-CD manual.[6]

Actual boundary values for the specific intersection under consideration, namely, Number 6 Shaft North at Hartebeestfontein Gold Mine Ltd, are used in the study. The inlet boundary conditions are specified as the inlet of 7.4 m/s at the duct inlet and a small inward velocity, approximately 0.14 m/s, at the top of the plenum to allow for the extra 50 m^3/s of air monitored at the bottom of the existing shaft. The outlet at the model shaft bottom is specified by setting the gradients of the velocity components to be zero. The boundary condition at the walls of the shaft and duct is specified as zero velocity and finally, at the symmetry plane, the normal gradients of the flow and the volume flow rate are specified as zero.

Results

A non-dimensional power loss coefficient is derived to depict the influence of the variable geometry parameters on the power loss over the intersection. This is done to ensure that the data can be used through interpolation and extrapolation for intersections with similar geometries but different flow conditions. The result obtained from the numerical model, which is needed to calculate the power loss coefficient, is the pressure at three locations in the model. The pressure at each location is taken as the integrated value of the pressure over the section. The three integration locations, or sections, are shown in Figure 4. The non-dimensional power loss coefficient for the fan drift-mine shaft intersection is:[7]

$$\Lambda_{\text{inters}} = \frac{(P_{T_1} - P_{T_3})\,\beta_{13}}{\frac{1}{2}\rho\overline{U}_3^2} + \frac{(P_{T_2} - P_{T_3})\,\beta_{23}}{\frac{1}{2}\rho\overline{U}_3^2} \qquad (3)$$

where the subscripts 1, 2, and 3 denote the position indicated in Figure 4; $\beta_{n3} = Q_n/Q_3$, the flow ratio at station n; P_{Tn} = total pressure at station n; and ρ and U are the density and average velocity, respectively. Although the derivation of the equation required the density to be constant, the solutions were obtained with the density being calculated at each node.

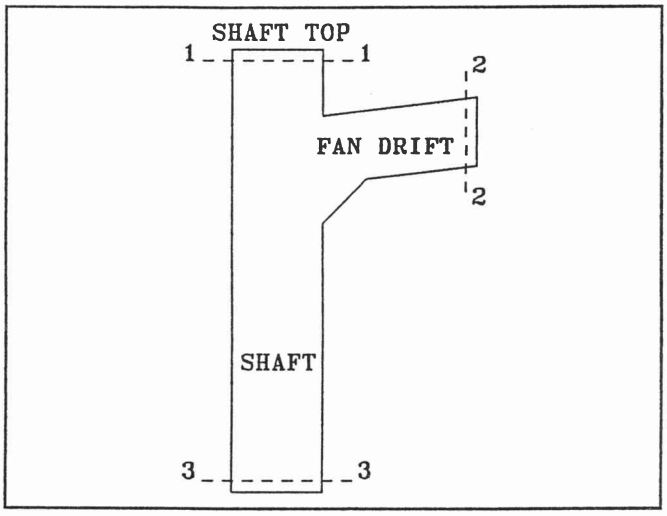

Figure 4. Locations where results are obtained.

The power loss coefficient is calculated for each case study, and the results are presented in Figures 5–8. For each of the three different slope angles (ϕ), a graph is plotted of the power loss coefficient against the duct angle (θ), producing three curves, for each ratio of length L to L_{original}. A separate graph is plotted for the case where $L/L_{\text{original}} = 0$, as the slope angle ($\phi$) is 90° at this setting of L and thus cannot be included in one of the other graphs.

Considering these graphs, a few tendencies are immediately evident. These tendencies are the following:

- The relationship between the power loss coefficient and the duct angle is approximately linear.
- The gradient of the curves changes from positive to negative for a slope angle between 45° and 67.5°.
- The power loss coefficient is reduced drastically when a slope in the duct floor is introduced.

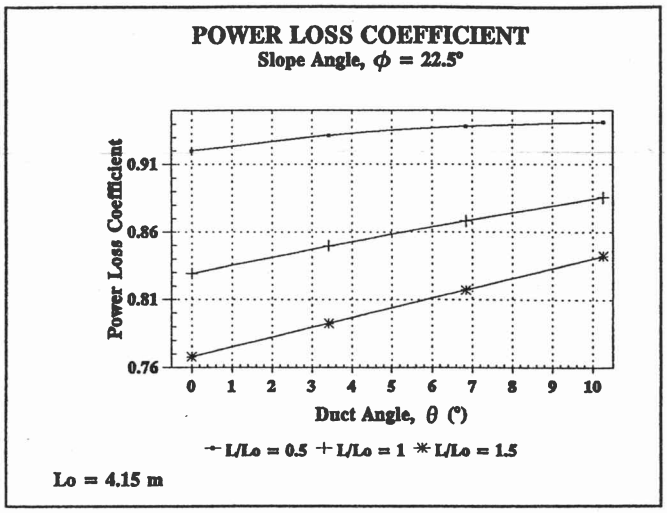

Figure 5. Power loss coefficient for case studies with $\phi = 22.5°$.

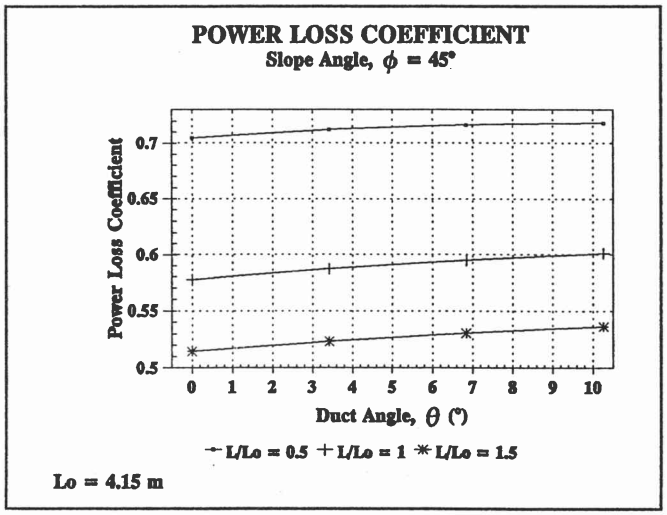

Figure 6. Power loss coefficient for case studies with $\phi = 45°$.

The energy loss across the intersection is found by multiplying the power loss coefficient with a constant term. Therefore the percentage reduction or increase in the power loss coefficient is the same as the percentage reduction or increase in the energy loss across the intersection. These percentages of increase or decrease in pressure loss are shown in Table 2, where values with a negative sign indicate a decrease in the pressure loss and these geometries are thus superior to the original geometry. From this table, it can be seen that case study 1 results in the largest increase in pressure loss. These geometries are shown, along with the original geometry (case study 24), in Figure 9.

The tendencies recognized in the graphs have to be explained to produce a better understanding of the behaviour of the flow in the different intersection geometries. Therefore, what does the change in sign of the gradient of the above curves imply? Firstly, it is obvious that a slope angle exists for which the duct angle between 0° and ± 10.5° would have virtually no effect on the power loss across the intersection. The change in sign is explained by considering the location in the intersection where the major pressure loss occurs. These locations can be seen in Figure 10.

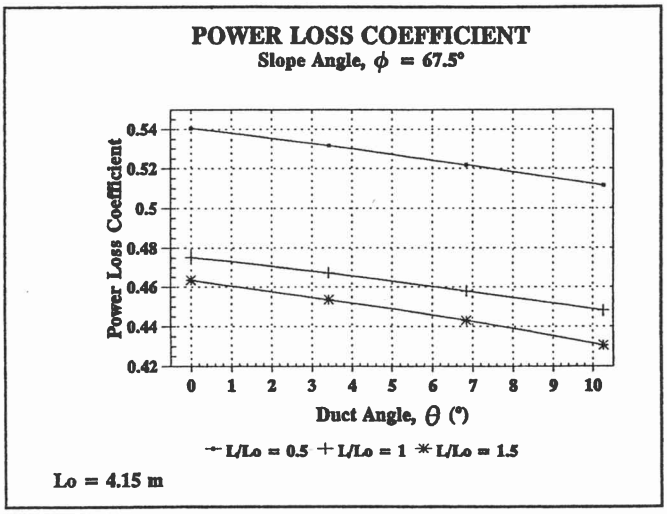

Figure 7. Power loss coefficient for case studies with $\phi = 67.5°$.

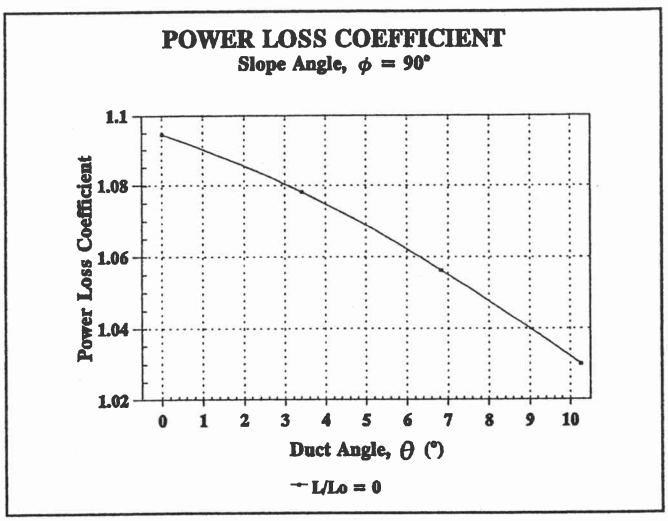

Figure 8. Power loss coefficient for case studies with $\phi = 90°$.

In the cases where the slope angle is lower than or equal to 45°, the major pressure loss occurs at the junction of the slope and the shaft wall. If a duct angle of 0° is specified, a large part of the pressure loss already occurs at the slope-duct junction, and the lowest total pressure loss over

Table 2 Percentage increase or decrease in pressure loss across the intersection

Case	% Change	Case	% Change	Case	% Change	Case	% Change
1	84.0	**11**	57.7	**21**	−1.3	**31**	−22.1
2	81.2	**12**	20.4	**22**	−21.5	**32**	33.2
3	77.5	**13**	−12.3	**23**	46.0	**33**	−12.1
4	73.1	**14**	58.2	**24**	0.0	**34**	−23.8
5	54.6	**15**	20.7	**25**	−23.0	**35**	37.4
6	18.4	**16**	−14.0	**26**	48.9	**36**	−10.8
7	−9.1	**17**	39.4	**27**	1.1	**37**	−25.5
8	56.6	**18**	−3.0	**28**	−24.7	**38**	41.6
9	19.7	**19**	−20.1	**29**	29.0	**39**	−9.8
10	−10.6	**20**	42.8	**30**	−13.5	**40**	−27.6

the intersection is obtained. In the cases where the slope angle is larger than 45°, the major pressure loss location is at the slope-duct junction. In these cases, the smaller the duct angle that is specified the higher the pressure loss at this point and from there the related increase in the total pressure loss. The changes in sign of the gradients seem to be at a slope angle higher than, but close to, 45°. The optimum slope angle seems to be close to 67.5°, but can only be presumed to exist between 45° and 90°. This optimum slope angle should ideally not cause any back flow areas or areas of very low velocity. The slope and duct angles are, however, not the only parameters that affect the pressure loss. The length, L, also plays an important role and should definitely be taken into account.

A tendency of the curves for the various lengths, L, is that the curves for different lengths tend to approach each other as the length increases. This shows that the length, L, has an optimum value, considering its effect on the power loss, for each slope angle, ϕ. If Figure 7 is considered, it can be seen that for this slope angle, the effect of increasing the length to 6.225 m has a relatively small influence on the power loss coefficient. Taking the construction cost and structural impact into account, this increase in the length, L, will probably not be feasible. Concluding, if the spectrum of geometries with their associated power coefficients is looked at, the most promising result is the pressure loss obtained with case study 13. The differences between this geometry and the original geometry are illustrated in Figure 11. This geometry gives a 12.3% reduction in the power loss, which is moderate compared to the 27.6% reduction of case study 40. It will therefore definitely be questioned why case study 13 seems to hold great promise?

The structural impact of the favourable geometry would be approximately the same or even less than that of the original geometry. If a geometry, such as that of case study 13, is to be implemented at the intersection, the location of the slope-shaft junction can be kept at the same position, as well as the duct itself. The only parameter that will have to be changed is the length, L, producing the optimum slope angle ϕ. This can actually be done by filling cement into the existing slope to achieve the desired geometry. The small change in geometry is evident from Figure 11. Although this geometry is not the optimum, it shows that a significant reduction in pressure loss can be achieved with a smaller slope area.

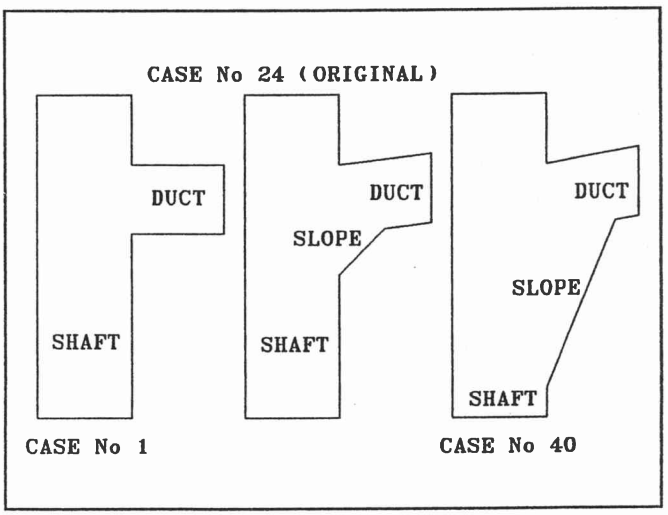

Figure 9. Geometries resulting in the highest increase and decrease in pressure loss.

Financial impact

To convert the reduction in power loss to the saving encountered, is an important part of the study. If no aerodynamic problems such as excessive shaft cross winds, air spilled to the atmosphere, etc. exist at a fan drift-mine shaft intersection, the saving in power cost achieved by the optimization, would be the only motivation to change an existing geometry. Although case study 13 is put forward as the most promising of those tested, the percentage reduction in power loss which is used in calculating the possible saving is taken as that of case study 40. This

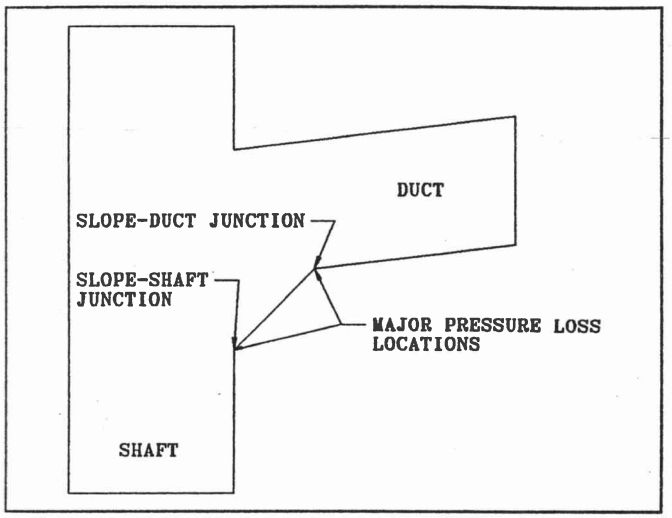

Figure 10. Major pressure loss locations.

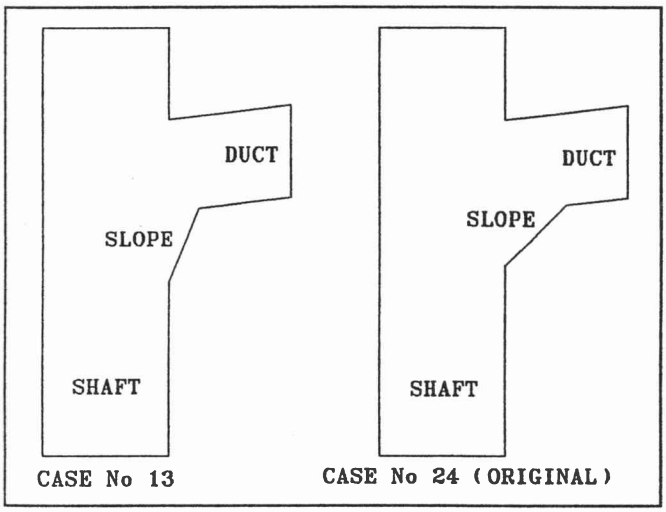

Figure 11. Differences between case study 13 and the original.

percentage reduction is used because it is felt that, with interpolation/extrapolation of the data obtained, a feasible alteration to the existing geometry can be determined to result in such a reduction. This saving in fan-power cost is calculated as follows: The air flow through the specific intersection is measured as 500 m^3/s. Every pascal pressure loss through the specific intersection, therefore presents an air-power loss of 0.5 kW (air power = pressure $\times$ volume flow). The average power cost, obtained from the Environmental Engineer at Hartebeestfontein Gold Mine, is R0,10/kWh (1 USA \$ $\approx$ R3) and the fan efficiency is taken as 60%. The power cost per annum, associated with one pascal pressure loss is R730.

The difference in pressure loss between case 24 and case 40 is 8.9 Pa. This pressure loss results in a saving of R4938 per annum. The capitalized present value of the saving over a period of 10 years, at a real interest rate of 10%, which is the difference between the loan interest rate and the inflation rate, is R170 000.

The saving in fan-power cost is more than three times higher than the cost of the CFD study, which is in the order of R50 000 for this size of study. This is a relatively small saving if the construction cost needed to obtain this saving is considered. Why is the saving encountered by a $\pm$ 28% reduction in pressure loss so small, as 28% seems to be a considerable reduction in pressure loss? If the calculation of the saving is considered, only two quantities can be increased to obtain a higher saving.

Either the difference in pressure loss, or the annual cost per pascal pressure loss, should be increased. This resolves to one parameter, namely, the volume flow rate. If a volume flow rate of 2 000–2 500 m^3/s present in most mines is considered, a much larger saving will result if all the fan drifts on a mine are optimized. With the same reduction in pressure loss, a volume flow rate of 2 500 m^3/s results in a saving of R850 000, which is also the capitalized present value at an interest rate of 10% over a ten-year period. A feasibility study will have to be done to determine the financial impact of such alterations and therefore if the saving in fan-power cost would justify the cost of the alterations. Another factor is the fact that all the intake shafts and ducts on a mine are not geometrically the same and that different studies may have to be done to find each optimum geometry.

Conclusion

The optimum geometry would be a curve instead of a slope at the intersection. But the cost and difficulty of building a curve, at the intersection, often constrain the designer to design a slope instead of a curve. Although a slope angle of 45° seems to be the obvious choice to simulate a curve at the intersection, this study showed that significant improvements in the aerodynamics can be made with a higher slope angle.

Concluding on the study as a whole, the outcome is illuminating in the percentage reduction by using only fixed ratios of the existing geometry parameters. It is proved inevitably that the existing methods of fan drift design are not incorrigible as far as aerodynamics are concerned. A fast, economically viable and effective method of optimizing the aerodynamics of a fan drift-mine shaft intersection is clearly found in CFD. Even if an intersection is built as a curve, the optimum radius is still unknown and should be optimized.

The somewhat disappointing saving in power cost, which was calculated as R6 486 per annum, is cancelled by the fact that a high percentage decrease in power loss across the intersection was obtained. This saving in power loss can result in enormous savings in intersections with higher volume flow rates. The saving, calculated with a

volume flow rate of 2 500 m^3/s, is approximately 16 times higher than the cost of the CFD study, making the method very attractive.

References

[1] Bonnington ST & Young GAJ. Some model studies of mine shafts, shaft insets and fan drifts. *Journal of the Mine Ventilation Society of South Africa,* 1962, **15**(5), pp.77–99.

[2] Eschenburg HMW. Scale model testing on upcast shaft bends and fan installations. *Journal of the Mine Ventilation Society of South Africa,* 1982, **35**(6), pp.41–45.

[3] Kroon A. Exit and entrance pressure losses at ventilation shafts. *Journal of the Mine Ventilation Society of South Africa,* 1963, **12**, pp.16–21.

[4] Nissen CJ. Design of shaft bends at Bafokeng South. *Journal of the Mine Ventilation Society of South Africa*, 1990, **43**(1), pp.9–13.

[5] Wrigley DE. Scale model testing of Erfdeel, mine opcast shaft bend and fan drift. *Journal of the Mine Ventilation Society of South Africa*, 1987, **40**(4), pp.49–53.

[6] STAR-CD. User's manual. Computational Dynamics, England, 1990, Version 2.111.

[7] Marx WM. *The minimizing of pressure losses in a fan drift-mine shaft intersection, using computational fluid dynamics.* MEng thesis, Potchefstroom University for CHE, 1992, pp.40–42.